

Electronic Supporting Information (ESI)

Structural and light coupling characteristics of patterned silica-titania sol-gel thin films with/without nano gold coating

Saswati Sarkar¹, Rik Chattopadhyay² and Sunirmal Jana^{1*}

¹Sol-Gel Division and ²Fibre Optics and Photonics Division

CSIR-Central Glass and Ceramic Research Institute (CSIR-CGCRI)

196 Raja S.C. Mullick Road, P.O. Jadavpur University, Kolkata 700032, West Bengal, India

C-O-N-T-E-N-T-S

| Section/Figure/Table | Page No. |
|--|----------|
| S1.0 Precursor sol and 1D/2D gel film | 2 |
| S2.0 UV-Vis absorption spectra | 3 |
| S3.0 FTIR spectra | 3 |
| S4.0 Diffraction pattern and diffraction efficiency | 4 |
| S5.0 FDTD simulation | 4 |
| Fig. S1: (a) Plot of viscosity versus ageing time, (b) plot of AFM peak height as a function of imprinting time and (c) load vs. depth curve of the gel film measured by nanoindentation technique. | 5 |
| Fig. S2: AFM images of the well-ordered 1D (i) and 2D (ii) patterned films (deposited from the sol of an optimum viscosity, ~2.35 cP) with applied pressure (~1.273 Pa). The corresponding line scan profiles are shown in (a) and (b), respectively. High fidelity stripe and square pillar-like patterns are observed from the AFM images. AFM image (~60 μm x ~60 μm) of 1D patterned film cured at 500°C (iii). | 6 |
| Fig. S3: UV-Vis absorption spectra of (a) solution having acetylacetone and solvents and (b) ST film on silica glass cured at 500°C. (c) Shows the reflectance spectra of different films cured at 500°C. | 7 |
| Fig. S4: Substrate corrected FTIR spectra of ST film cured at different temperatures. | 7 |
| Fig. S5: XRD reflections of (a) silica-titania (ST) thin film cured at 150°C and 300°C along with (b) ST film cured at 500°C and Au coated silica-titania thin film (Au-ST). | 8 |
| Fig. S6: Diffraction patterns of patterned silica-titania thin films: (a) and (b) are the generated diffraction patterns from AFM-First Fourier Transform (FFT) for 1D and 2D, respectively. (c) and (d) show the photographs of experimentally observed diffraction patterns on screens for 1D and 2D, respectively. | 8 |
| Fig. S7: Scheme for the experimental optical set up to measure angle of diffraction and diffraction efficiency of patterned films. | 9 |
| Fig. S8: Schematic diagram showing the sensor designs of (a) 3-layer waveguide and (b) 4-layer surface plasmon waveguide | 9 |
| Fig. S9: FDTD solutions: (a) Normalized power output of 2D patterned film, (b) SP mode confinement with (c) SP coupled normalized output power in 60 nm thick Au layer over GL of 1D patterned thin film (GL thickness, 175 nm; RI 1.788). Respective GL thickness is embedded in the figure. | 10 |
| Table S1: Ellipsometric data of silica-titania film cured at different temperatures | 11 |
| Table S2: Diffraction efficiency data of 1D patterned film | 11 |

S1.0 Precursor sol and 1D/2D gel film

The viscosity of 1h aged precursor sol was found to be ~ 1.97 cP. However, the viscosity of the sol was noticed to gradually rise with sol aging time. It was observed that after 72 h ageing, the sol viscosity reached to ~ 3.2 cP. The embossing of the as-deposited film deposited from the sols of different ageing time (1 h, 4 h, 24 h, 36 h, 48 h and 72 h) using the PDMS stamp having negative replica of the 1D pattern of master CD. The fidelity of the grating film was checked with measured AFM surface topographies along with their corresponding height profile (HP). It can clearly be seen from Fig. S1a that high fidelity and well-ordered 1D pattern having maximum HP formed from the precursor sol with an optimized viscosity of ~ 2.4 cP for 4h aged precursor sol.

It is also noted that the time of 2nd imprinting for creation of 2D pattern (Fig. S1b) was optimized to 45 min from time of 1st imprinting to obtain high fidelity and well-ordered 2D pattern of relatively high value in HP. It is worthy to note that an external pressure was applied during the 2nd imprinting. In this respect, we varied the 2nd imprinting time and after 45min of the 1st imprinting, we obtained a high fidelity and well-ordered 2D pattern. As the gel film is a soft material which could deform under excess applied pressure as confirmed from the load versus depth plot (Fig. S1c), constructed from nanoindentation data.¹ From the plot, it could realized that the gel film is an elastoplastic in nature.^{2,3} This could easily be realized by simple mechanistic calculations. In this calculation, the optimum deformation range of the soft gel film found to be in terms of asperity contacts in the order of ~ 19.7 μm but with the increase of the applied pressure, there might be a simple increase in local stress or asperity deformation induced enhancement in the local stress further. In both cases, the material could fail as the stress was much higher than the yield stress which the soft gel material could bear. With increasing the pressure enriching the optimum, the system fails to hold its integrity further. This elastoplastic property of gel film could effectively help to fabricate crack free 2D structure under the applied external pressure. If the nature of gel film became only plastic, then it would deform at the time of 2nd imprinting process but no such deformation in surface patterned structure was found in the 2D patterned film when applied pressure was ~ 1.27 Pa. However, structural deformity in the 2D pattern was observed at relatively higher applied pressure or a longer 2nd imprinting time. Therefore, the time and applied external pressure for the 2nd imprinting were very important

aspects making 2D surface patterned film. It is important to note that the high fidelity 2D structure onto the film surface remained unaffected even in the thermally cured film 500°C.

S2.0 UV-Vis absorption spectra

UV-Vis absorption spectra (Fig. S3a,b) of as-deposited film showed a strong UV absorption peak at ~300 nm (Fig. S3b) but the solution having the solvents and acetylacetonone (acac, kept similar with the precursor sol) without the alkoxides showed the absorption peak at ~270 nm (Fig. S3a). This UV peak could be originated from the π - π^* transition of acetylacetonone.⁴ However, the red shifting of the UV peak could imply the formation of acac complex of metal ions [Ti(IV)] present in the film matrix.⁵ Therefore, the function of acac as stabilizing/complexing agent is confirmed from the study of UV-Vis spectra of the samples.

S3.0 FTIR spectra

Figure S4 shows the FTIR spectrum of the film cured at different temperatures. The spectrum shows the characteristics FTIR peaks ~ 1585 and 1526 cm^{-1} , attributed to asymmetric stretching vibrations of $\nu(\text{COO}^-)$ and $\nu(\text{C-H})$, respectively, implying the bidentate chelating character of acetylacetonone with the metal ions [Ti(IV)/Zr(IV)] of the as-deposited gel film. The sample also shows the existence of prominent vibrations at 1458 and 1358 cm^{-1} , assigned to the asymmetric stretching of $\nu(\text{CH}_3)$ and symmetric out of plane bending of $\delta(\text{CH}_3)$ from the organic part of metal alkoxides used for the preparation of precursor sol.⁶ The FTIR vibrations in the spectral region, 1300-950 cm^{-1} could be responsible due to homonuclear Si-O-Si and heteronuclear Si-O-Ti present in the gel film.^{6,7} However, all the vibrations appeared due to the presence of organics became disappeared when the film was cured at 500°C. It is known that with increasing the curing temperature, more and more hydrolysis and condensation reactions could occur in the gel film material, resulting the formation of Si-O-Ti linkage.⁸ The peaks appeared at ~970 and ~940 cm^{-1} became prominent in the 500°C cured film for the formation of Si-O-Ti bond in the oxide film material.^{8,9}

S4.0 Diffraction pattern and diffraction efficiency

It is known that film surface periodic structure could couple light and enhance the light guiding efficiently in an optical waveguide medium.¹⁰ In this work, we measured the diffraction efficiency of the patterned film. For this study, to obtain fixed intensity from the light source (He-Ne laser, 632.8 nm), it was left on for about 1 h before the measurement. From Figure S6 (c,d), it can clearly be seen that a centre dot (0th/ fundamental order) appears along with two set of dots for 1st order (+1 and -1) and 2nd order (+2 and -2), respectively in a horizontal line for 1D pattern film whereas the 2D patterned film generated two set of diffraction order appeared as a centre dot (0th/ fundamental order) along with four dots as 1st order (+1 and -1) and 2nd order (+2 and -2) for the film cured at 500°C. On the other hand, one of the main characteristics of gratings/patterns is the diffraction efficiency, η in terms of power throughput. In this measurement of η , the calculation were done by considering the initial power output of the source of 2.7 mW. Moreover, we measured by collecting the output power via a detector connected to a powermeter by keeping the distance between the light source to sample and sample to detector fixed.

S5.0 FDTD simulation

Optical fibers and channel waveguides could provide confinement of light in two dimensions which perhaps causes bending and dispersion losses respectively.¹¹ The fabricated patterned dielectric silica-titania (ST) film could act as a grating coupled sensor of three layer waveguide; glass substrate (acts as clad, RI 1.4546), ST film (as guiding layer, RI 1.788) having high fidelity pattern (HP ~30 nm, periodicity 1.5 μm) that could help to couple light and air (as cover layer, RI 1.0). Theoretical simulation of the waveguide sensor structure was performed by using Finite Difference Time Domain, FDTD software (Lumerical FDTD Solutions 8.7.1) for patterned ST film. In this simulation, we considered, substrate thickness of 1.03182 μm with refractive index, n_s of 1.4546, film guiding layer d_f of 100-200 nm with refractive index $n_f = 1.788$, pattern height ~32 nm, pitch (periodicity) $\Lambda = 1.5 \mu\text{m}$, cover layer (air) $n_c = 1$ with thickness 1 μm , light source operating wavelength $\lambda = 632.8\text{nm}$ (red light). Moreover, the FDTD simulation was carried out for nano Au coated patterned waveguide (all the simulation parameters kept same as used for ST patterned films). This would behave as a four layer plasmonic waveguide consisting of substrate ($n_s = 1.4546$), patterned guiding layer ($n_f = 1.788$), Au layer ($n_m = 1.323$) and cover layer (air, $n_c = 1$).

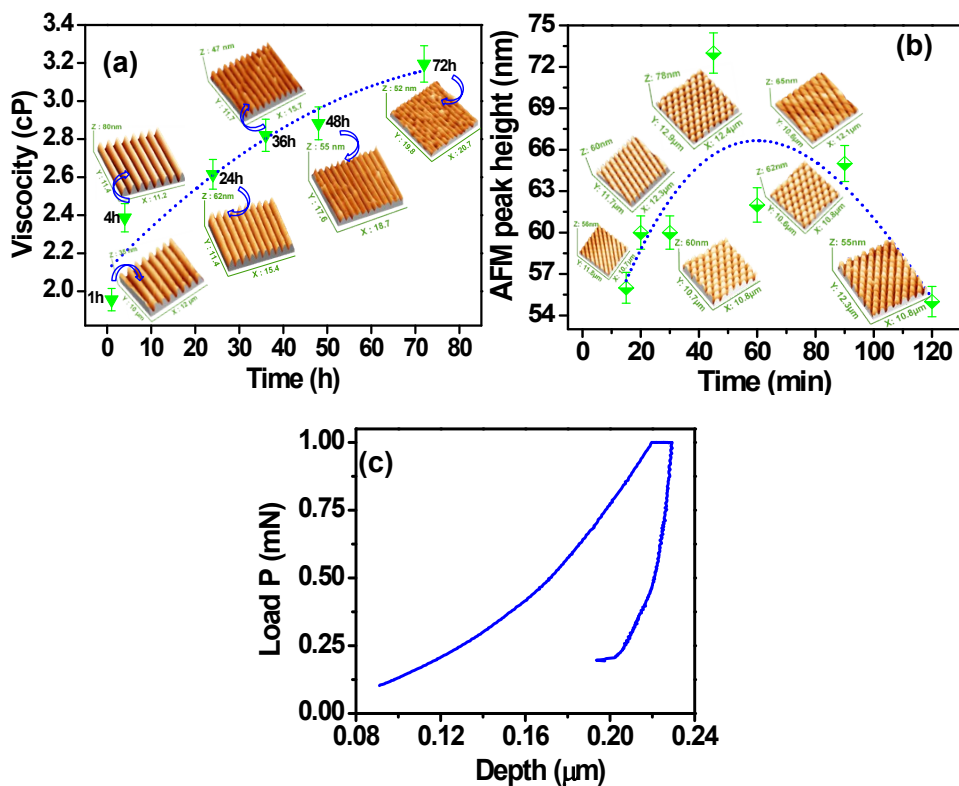


Fig. S1: (a) Plot of viscosity versus ageing time and (b) plot of AFM peak height as a function of imprinting time (the AFM images of 1D or 2D patterned films at the corresponding imprinting time are embedded in the figures). (c) Load vs. depth curve of the gel film measured by nanoindentation technique (the measurement was done after ~50 min of the film deposition)

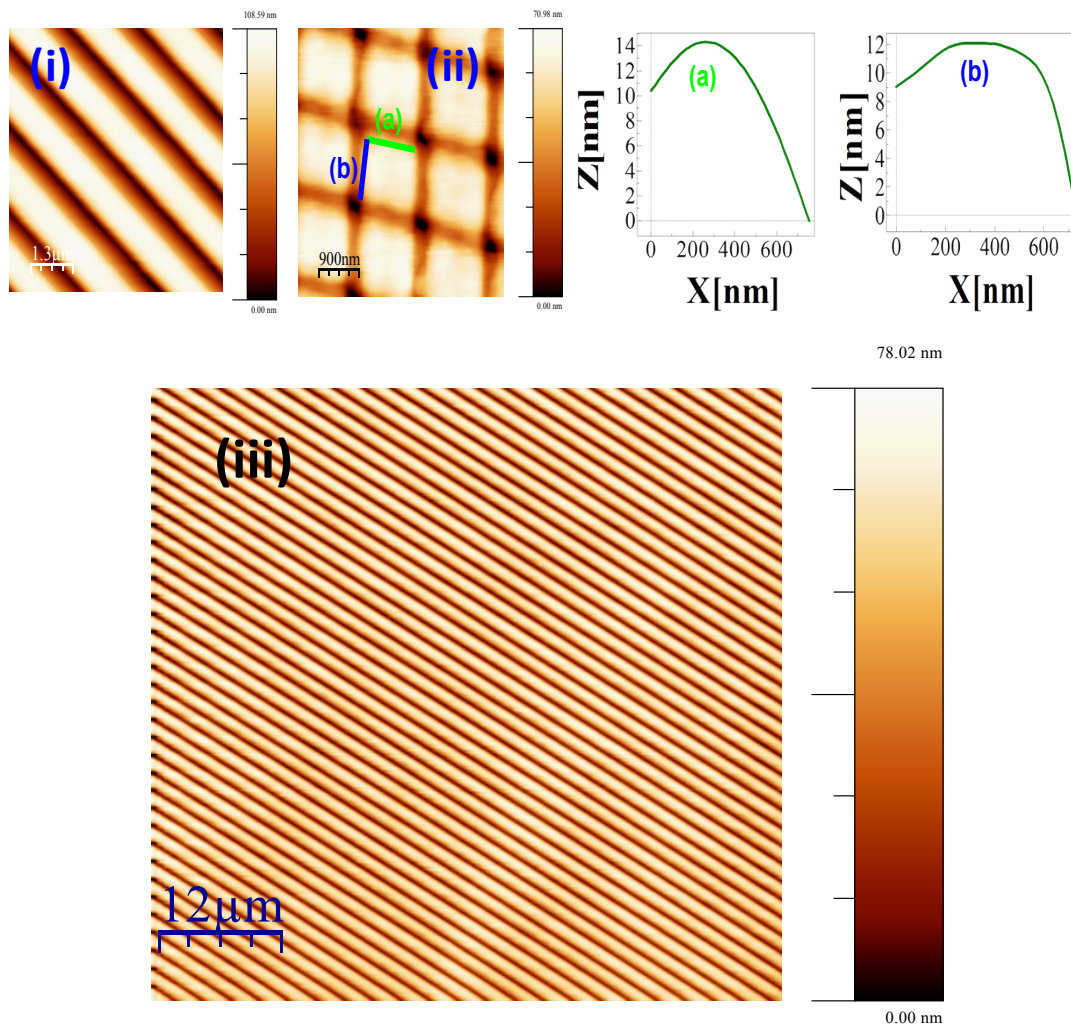


Fig. S2: AFM images of the well-ordered 1D (i) and 2D (ii) patterned films (deposited from the sol of an optimum viscosity, ~ 2.35 cP) with applied pressure (~ 1.273 Pa). The corresponding line scan profiles are shown in (a) and (b), respectively. High fidelity stripe and square pillar-like patterns are observed from the AFM images. (iii) AFM image ($\sim 60 \mu\text{m} \times \sim 60 \mu\text{m}$) of 1D patterned film cured at 500°C .

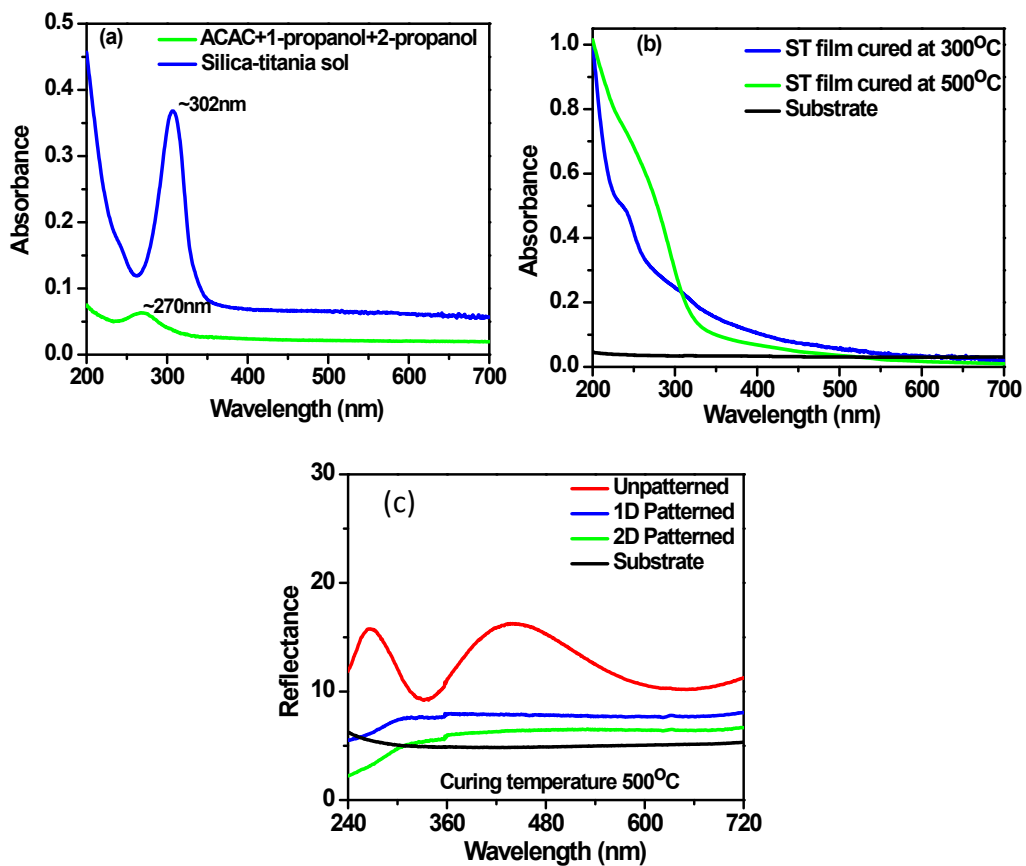


Fig. S3: UV-Vis absorption spectra of (a) solution having acetylacetone and solvents and (b) ST film on silica glass cured at 500°C. (c) Shows the reflectance spectra of different films cured at 500°C.

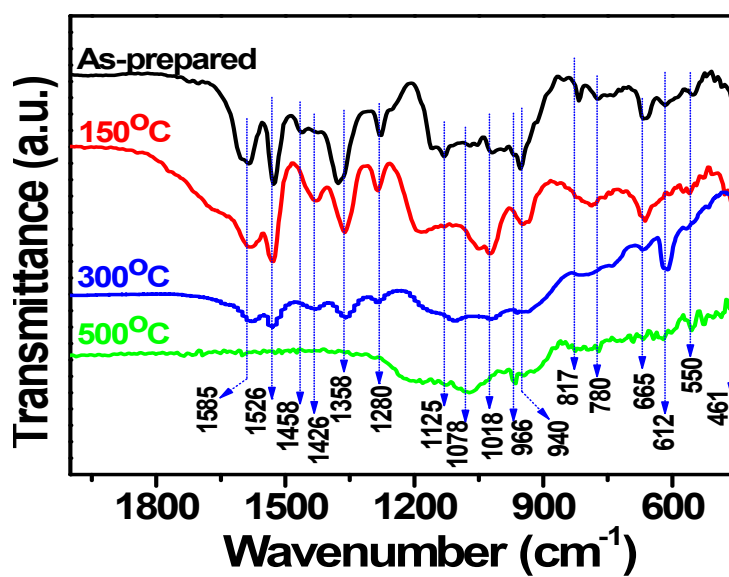


Fig. S4: Substrate corrected FTIR spectra of ST film cured at different temperatures.

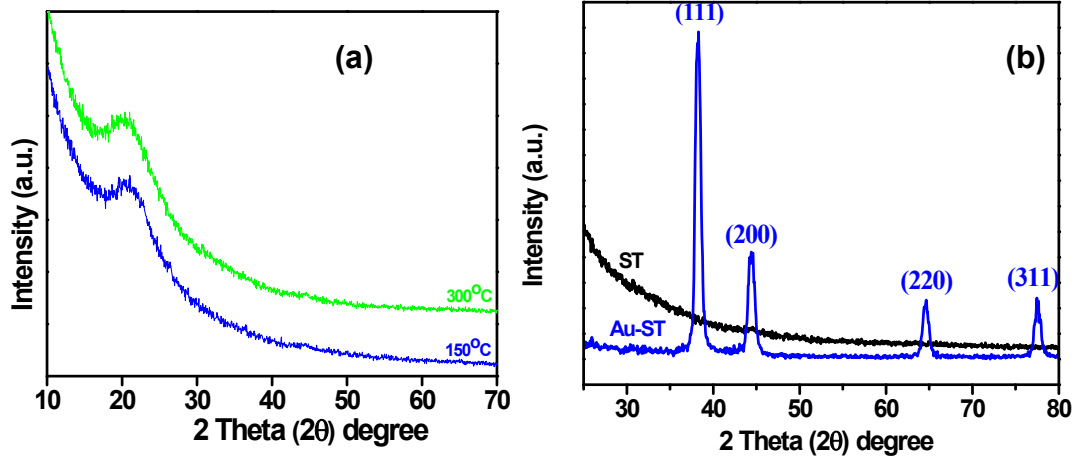


Fig. S5: XRD reflections of (a) silica-titania (ST) thin film cured at 150 °C and 300 °C along with (b) ST film cured at 500°C and Au coated silica-titania thin film (Au-ST).

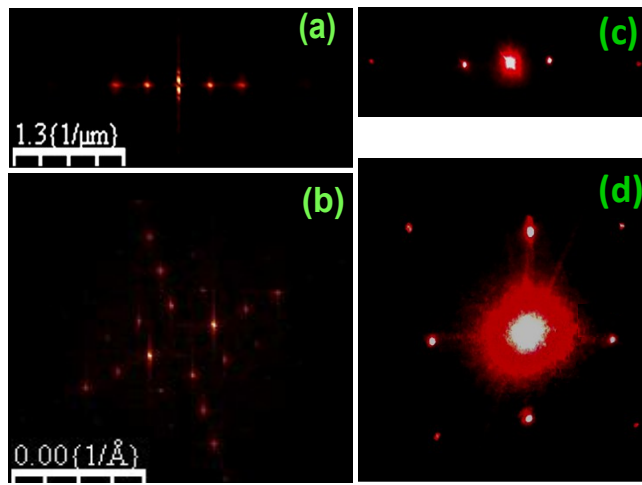


Fig. S6: Diffraction patterns of patterned silica-titania thin films: (a) and (b) are the generated diffraction patterns from AFM-First Fourier Transform (FFT) for 1D and 2D, respectively. (c) and (d) show the photographs of experimentally observed diffraction patterns on screens for 1D and 2D patterned films, respectively.

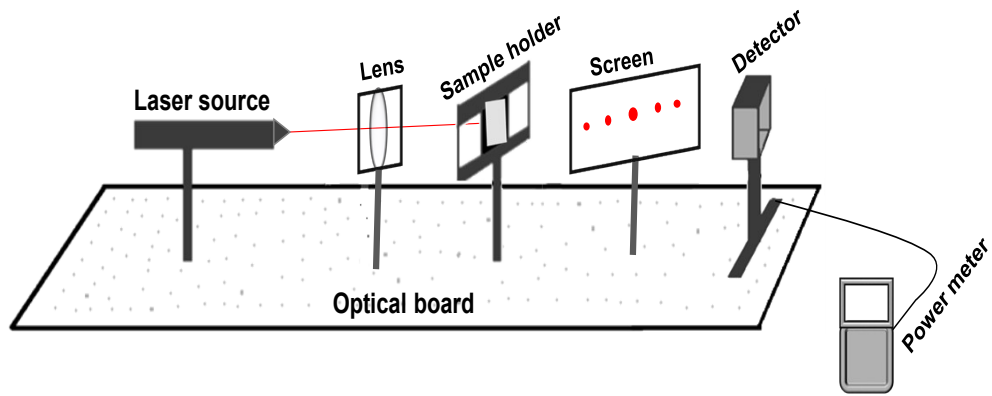


Fig. S7: Scheme for the experimental optical set up to measure angle of diffraction and diffraction efficiency of patterned films.

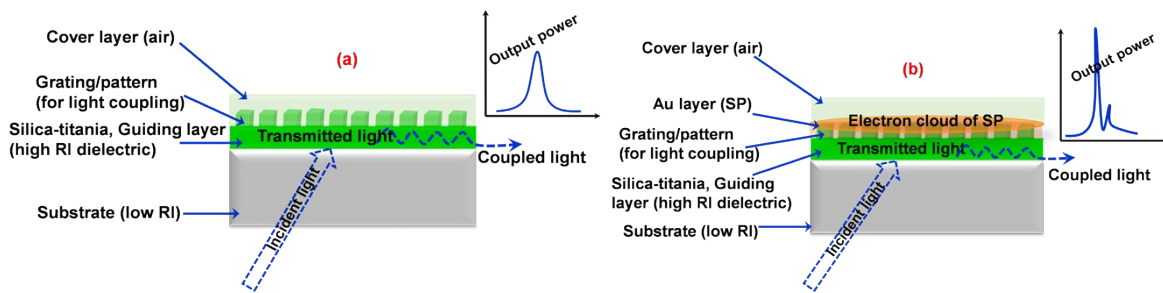


Fig. S8: Schematic diagram showing the sensor designs of (a) 3-layer waveguide and (b) 4-layer surface plasmon (SP) waveguide

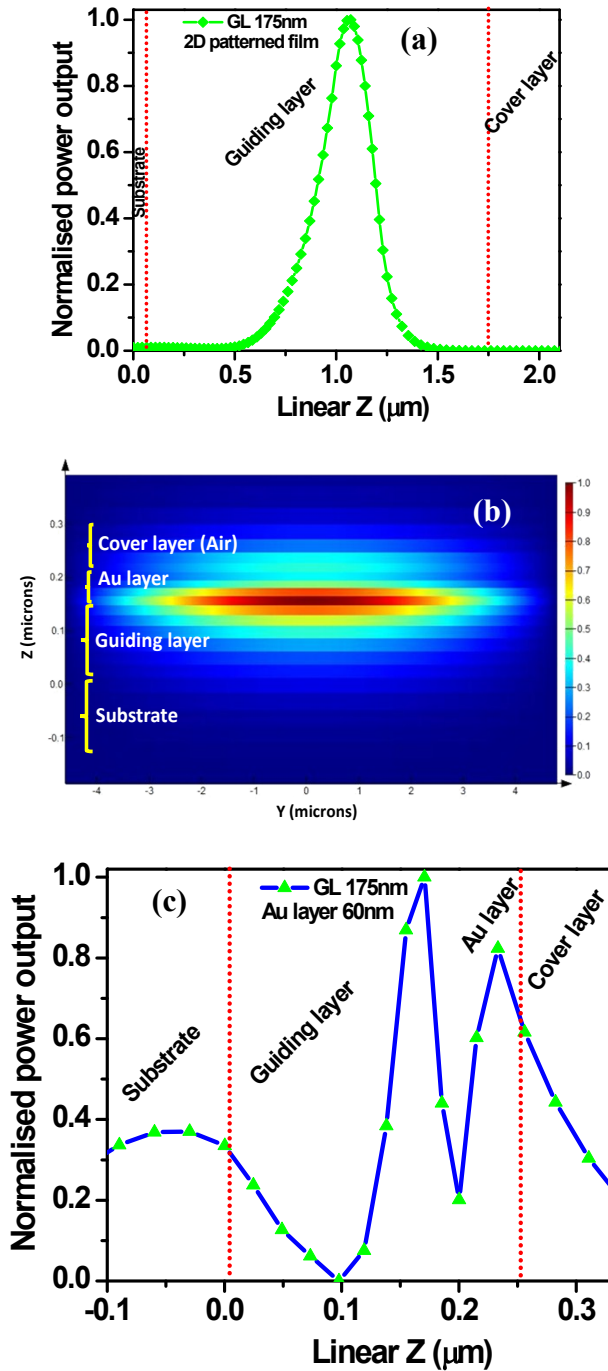


Fig. S9: FDTD solutions: (a) Normalized power output of 2D patterned film, (b) SP mode confinement with (c) SP coupled normalized output power in 60 nm thick Au layer over GL of 1D patterned thin film (GL thickness, 175 nm; RI 1.788). Respective GL thickness is embedded in the figure.

Table S1: *Ellipsometric data of silica-titania film cured at different temperatures*

| Curing temperature (°C) | Thickness (± 1.5 nm) | Refractive index (± 0.003) | Calculated volume porosity, P (%) |
|-------------------------|-------------------------|-------------------------------|--------------------------------------|
| Ambient | ~240 | 1.656 | 29.75 |
| 150 | ~217 | 1.691 | 26.37 |
| 300 | ~195 | 1.725 | 23.67 |
| 500 | ~172 | 1.788 | 19.2 |

Table S2: *Diffraction efficiency data of 1D patterned film*

| Sl. No. | Diffraction order | Absolute diffraction efficiency, η_a (%) |
|---------|-------------------|---|
| 1. | 0 | 91.68 |
| 2. | +1 | 0.84 |
| 3. | -1 | 0.84 |
| 4. | +2 | 0.02 |
| 5. | -2 | 0.03 |

References

- (1) C. W. MacMinn, E. R. Dufresne and J. S. Wettlaufe, *Phys. Rev.*, 2015, **X 5**, 011020-(1-12).
- (2) S. Sarkar, S. K. Bhadra and S. Jana, *RSC Adv.*, 2016, **6**, 46048-46059.
- (3) P. E. Mazeran, M. Beyaoui, M. Bigerelle and M. Guigon, *Int. J. Mat. Res.*, 2012, **103**, 715-722.
- (4) R. Lozada-Garcia, Dynamics and photodynamics of acetylacetone in para-hydrogen matrices. Other [cond-mat.other], Universite Paris Sud - Paris XI, 2012, English. <NNT: 2012PA112380>. <tel-0780495>.
- (5) Y. Chena, Y. Huang, J. Xiu, X. Hana and X. Bao, *Applied Catalysis A: General*, 2004, **273**, 185-191.
- (6) I. Karatchevseva, D. J. Cassidy, Z. Zhang, G. Triani, K. S. Finnie, S. L. Cram and C. J. Barbe, *J. Am. Ceram. Soc.*, 2008, **91**, 2015–2023.
- (7) S. Jana, M. A. Lim, I. C. Baek, C. H. Kim and S. Seok, *Mat Chem. Phys.*, 2008, **112**, 1008–1014.
- (8) D. D. Lekeufack, A. Brioude, A. Mouti, J. G. Alauzun, P. Stadelmann, A. W. Colemana and P. Mielea., *Chem. Commun.*, 2010, **46**, 4544–4546.
- (9) P. R. Aravind, P. Shajesh, P. Mukundan and K. G. K. Warriar, *J. Sol-Gel Sci. Technol.*, 2009, **52**, 328-334.
- (10) K. Schmitt, C. Hoffmann, M. Zourob, A. Lakhtakia, (eds.), Springer, Verlag, Berlin, Heidelberg, 2010, DOI 10.1007/978-3-540-88242-8_2.
- (11) M. Niveiri and E. Popov, *Light propagation in periodic media; Differential theory and media*, Merce Dekker Inc., New York, 2003.